ChemComm

Force Fields for Water-Surface Interaction: Is Reproduction of the Experimental Water Contact Angle Enough?

Journal:	*ChemComm*
Manuscript ID	CC-COM-01-2021-000426.R2
Article Type:	Communication

COMMUNICATION

Force Fields for Water-Surface Interaction: Is Reproduction of the Experimental Water Contact Angle Enough?

Le Nhan Pham[a] and Tiffany Walsh*[a]

Received 00th January 20xx,
Accepted 00th January 20xx

DOI: 10.1039/x0xx00000x

A new protocol based on quantum chemical calculations and molecular dynamics simulations is proposed to revisit water-MoS_2 interfacial force fields (FFs). The accurate reproduction of experimental water contact angles is suggested to be insufficient to ensure reliable FFs for recovering structural properties of the interfacial solvent. As an example, this protocol is used to develop a new set of FF parameters to both capture interfacial structural phenomena at the interface between water and MoS_2 and recover experimental water contact angle data. This approach can be applied to any interface where contact angle data are available.

Measurement of water contact angles (WCAs) is a typical strategy to gauge the wettability of solid surfaces. A droplet of water stably maintained on a surface is a result of a complex balance of inter-solvent and solvent-interfacial interactions.[1,2] Characterization of WCAs provides valuable insights into the physico-chemical properties and surface structures of materials.[1,3]

From a classical perspective, stabilization of a water droplet on a surface can be attributed to the equilibrium of classical atomic forces. Therefore, the formation and stabilization of water droplets on surfaces can be theoretically probed via molecular dynamics (MD) simulations. Indeed, several MD simulation studies have reported different aspects of nanodroplets on materials surfaces, e.g. advancing and receding, hysteresis, and evolution dynamics.[4–6] In doing so, a force field (FF) with the capability to accurately capture the interfacial interactions between water and surfaces is of paramount importance. Therefore, during the process of FF parametrization, reproduction of accurate WCAs is usually a key criterion for FF assessment and/or validation, as reported for various interfacial FFs for materials such as graphene,[7] boron nitride,[8,9] molybdenum disulfide,[10–12] and silica.[13]

With a wide range of potential applications in biological sensors,[14,15] water treatment,[16–20] gas-sensing[21,22] and electronic devices,[23,24] nanosheets of MoS_2 and their interfaces are a subject of high interest. However, the challenge with MD simulation approaches is that a reliable and accurate FF to describe the interfacial interactions is not always available and may require development. Several FFs have been developed for simulating the MoS_2 nanosheet[25–27] and interfacial interactions between MoS_2 layers with water[10,11,28,29] and biomolecules.[12,30]

A typical step in assessing the reliability of newly developed interfacial FFs is to reproduce the experimental WCA.[10–12,28,29] The key question here is whether a set of different FFs that can each reproduce the experimental WCA can also support common structural traits of the interfacial solvent. Specifically, the structural trait of interest is energetic ranking of the different possible binding structures of the surface-adsorbed water. This ranking is relevant, because the structuring of the interfacial solvent is thought to strongly influence biomolecule adsorption.[31] Here, several FF parameter sets that can recover the MoS_2 experimental WCA are shown to support a range of different energetic ordering of water configurations on the MoS_2 surface, some of which substantially differ from the quantum chemical hypersurface. Therefore, this ordering is proposed as an additional new criterion to assess FF quality for water-surface simulations. Following these two criteria, a new set of parameters for the water-MoS_2 interface was developed.

The quantum chemical water-MoS_2 hypersurface was characterized using fifteen configurations of water adsorbed on the MoS_2 basal plane optimized at the vdW-DF2[32] level of theory using the Quantum Espresso 6.4.1 package.[33] This particular functional was selected on the basis of reproduction of the two available experimental adsorption energies for this material, thiophene and butadiene (benchmarking details in the ESI). The optimized configurations were subsequently used in part to inform and assess the FF parameters developed in this work and those reported previously.[10–12,28,29] All MD simulations were done with the Gromacs 2018.3 package.[34] Full details of method selection, quantum chemical calculations, MD simulations, and Lennard-Jones parameterization are provided in the ESI.

[a] *Institute for Frontier Materials, Deakin University, Geelong, Victoria 3216, Australia. E-mail: tiffany.walsh@deakin.edu.au*

Electronic Supplementary Information (ESI) available: Configurations of all remaining configurations; computational methods; effects of ZPE on adsorption energy; energetic orderings produced by using 5 sets of parameters and different water models. See DOI: 10.1039/x0xx00000x

The adsorption energy of water on the basal plane of MoS_2 was estimated to be ~15 kJ/mol. Several configurations were found to have close interaction energies, ranging from 13.0 to 15.0 kJ/mol. These values are in good agreement with theoretical adsorption energies reported elsewhere.[35,36] Geometrical structures of the strongest four binding configurations (C1-C4) are given in Figure 2.

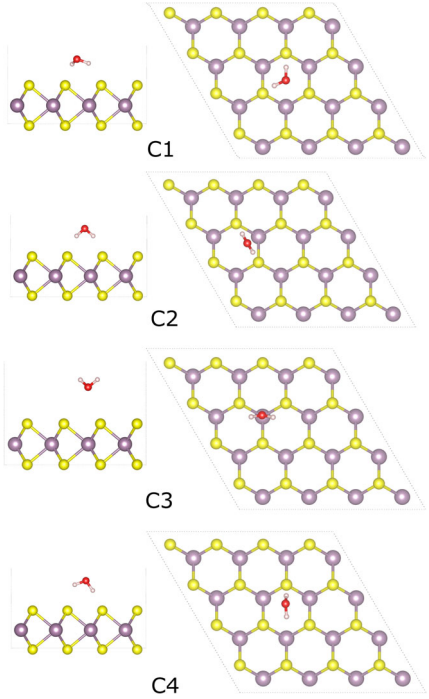

Figure 2 Side and top views of the four strongest binding configurations of water on the MoS_2 basal plane.

Table 1 Force-field parameter sets for MoS_2/water interactions that can reproduce experimental WCAs. The associated water models are provided in the last row. Corresponding FFs used for specific sets are CHARMM27 (S1-S5) and OPLSAA (S6).

para.	Parameter Set					
	S1[12]	S2[12]	S3[11]	S4[28]	S5[29]	S6[10]
σ_{Mo}	0.480	0.480	0.443	0.393	0.420	0.255
ε_{Mo}	0.293	0.293	0.485	0.192	0.254	0.544
σ_S	0.384	0.384	0.334	0.336	0.313	0.350
ε_S	1.255	1.255	2.085	1.121	1.484	1.046
q_{Mo}	+0.50	+0.50	+0.50	+0.60	+0.00	+0.76
q_S	-0.25	-0.25	-0.25	-0.30	-0.00	-0.38
water	TIP3P[37]	SPC[38]	SPC/E[38]	SPC/E	SPC/E	TIP3P

Six sets (S1-S6 in Table 1) of non-bonded FF parameters and water models taken from literature were used to calculate the interaction energies of these fifteen water-surface configurations. It is noted that sets S3 and S4 were actually fitted to the experimental water contact angle. Their energetic rankings, alongside those from the vdW-DF2 calculations and the FF from the current work (CW), are illustrated in Figure 1 (data provided in Table S4, ESI). Three classes of energetic rankings are apparent. Sets S1 and S2 (and to a lesser extent,

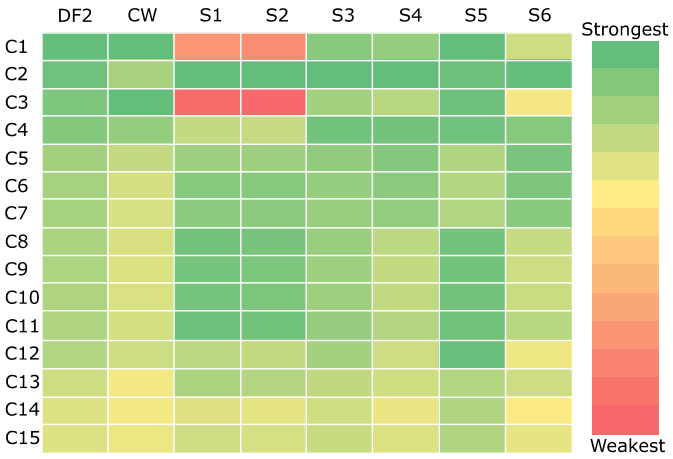

Figure 1 Energetic ordering of water configurations (C1-C15) adsorbed on the basal plane of MoS_2. S1 to S6 are orderings produced by the FF parameter sets and water models listed in Table 1. DF2 and CW are energetic orderings determined vdW-DF2 and the FF parameters of this current work, respectively.

S6) comprise the first category. These rankings are not in agreement with those produced by using the other sets (S3-S5). Specifically, two of the strongest-binding DFT configurations C1 and C3 were repulsive for the S1 and S2 sets (Table S4, ESI) suggesting these states would not likely appear in MD simulations of interfacial solvent structuring using FFs S1 or S2.

The second category comprises S3, S4 (and CW). These are in broad agreement with the vdW-DF2 rankings. It is noted that the S4 parameters were fitted to energies calculated using the reliable and robust random phase approximation (RPA) approach.[28] However, the S4 set were fitted to only a limited number (five) of RPA water-surface orientations, since these calculations are very intensive. Furthermore, the input geometries for these RPA calculations did not include any of the DFT-optimized configurations. This could be the reason why the S4 set cannot recover the strongest configuration C1. Although it is not the aim of the current work to propose a definitive energetic ordering, such agreement gives a vote of confidence to the DFT data, given the high reliability of the RPA approach to such weakly-bound systems. The remaining S5 rankings do not agree with any other data (Figure 2), indicating that several of the more weakly-bound DFT states (C8-C12) have strong surface interactions. This suggests that interfacial solvent structures using this the S5 FF would likely prominently feature these configurations at room temperature.

These data suggest that although different parameter sets can reproduce experimental WCAs,[10,12] they are not necessarily consistent in identifying the most and least important geometrical configurations of water on the MoS_2 surface. If the DFT and RPA data can be assumed to be a reasonably reliable description of the quantum hypersurface, then several of the FFs considered here may not be capable of capturing the dynamic structural ensemble of interfacial water on the MoS_2 surface. Note that with a similar evaluation procedure, any set of interfacial FF parameters could be re-assessed as long as contact angles are experimentally available. In summary, here we suggest a protocol based on satisfying both the quantum

hypersurface and experimental contact angles. This could be extended to other physical properties, such as the liquid/solid interfacial tension.[29] The reason why different microscopic ensembles can produce the same contact angle are clear; as remarked by Leroy[29], the process of inferring a set of force-field parameters that can satisfy a single macroscopic property cannot mathematically admit a unique solution, but rather an infinite family of solutions.

Our first attempt to fit the nonbonded parameters to the vdW-DF2 data points resulted in unstable water droplet simulations on the basal plane of MoS_2. However, just a small scaling in the interaction energy of the fitting data can yield stable droplets and a range of stable WCAs. This result reveals that contact angles are very sensitive to the energy range of the fitting set. The weak interaction (~15 kJ/mol) between water and MoS_2 is proposed to be the cause of this sensitivity. Therefore, any correction to the interaction energies of the fitting dataset can significantly influence water droplet stability. It is noted that the vdW-DF2 energies were initially fitted without any further correction, such as zero-point energy (ZPE) and/or the chemical accuracy of the vdW-DF2 functional.

For weak interfacial interactions, the ZPE correction can make a significant contribution. Indeed, by using cluster models of water-MoS_2 interaction (details in ESI), the ZPE was found to substantially reduce the water-MoS_2 binding energy. In addition, all interaction energies calculated using parameter sets S1-S6 are smaller than the vdW-DF2 energies (Table S4, ESI). Therefore, we propose that the ZPE is an important factor in the formation of water droplets. Since a ZPE correction to every water-MoS_2 configuration is impractical, and the errors in chemical accuracy of vdW-DF2 are not readily quantified, it was decided to fit non-bonded parameters within the framework of the CHARMM22* force field[39,40] to a *scaled* set of the DFT energies, such that the experimental WCA was recovered. Critically, the fitting process always ensures that the resultant parameters can recover the vdW-DF2 energetic ordering.

The new parameters (Table 2) describe the interaction between water (TIPS3P[37,41]) and the basal plane of MoS_2 and can recover the experimental WCA and energetic ordering of the water-surface configurations. The macroscopic WCA (θ) was extrapolated from WCAs of three different nanodroplet sizes (Figure 3), derived using Young's equation:

$$\cos(\theta) = \cos(\theta_\infty) - \frac{\tau}{\gamma_{LV}} r_B^{-1} \qquad (1)$$

where γ_{LV} is the water liquid-vapor surface tension, r_B is the droplet base radius, and τ is the line tension. Using the extrapolation procedure of Werder et al,[42] the macroscopic droplet contact angle was then calculated to be 70°, very close to the experimentally reported early WCA of 69°.[43] From the energetic ordering of water-surface configurations obtained from this newly fitted set (denoted CW in Figure 1), this FF can recover the strongest configuration C1 and several other low-energy states (C2-C5). Furthermore, quantum chemically unfavourable configurations (C13-C15) are also consistently identified by this new FF. These two crucial features, reproduction of the energetic ordering and the experimental contact angle, make these new interfacial FF parameters quantitatively capable of predicting the structural and dynamic interfacial behaviours of water on the MoS_2 surface. It is noted that parameter sets S3 and S4 yield performance consistent with the CW set. However, unlike S3 and S4, the new CW set is designed to be harmonized with the CHARMM22* FF, to enable future inclusion of biomolecules into this parametrization. Another clear difference between the CW parameters and S1-S6 is that the CW set fitted bespoke surface-oxygen and surface-hydrogen interactions, whereas S1-S6 used mixing rules. It is possible that such separation of treatment allows recovery of the strongest interaction configuration C1 (Figure 1).

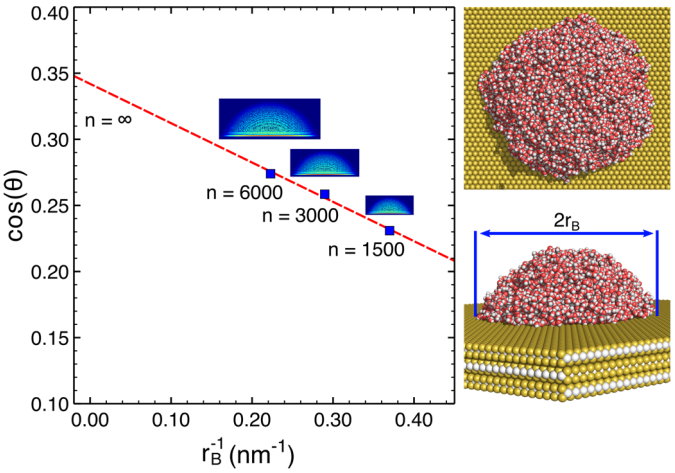

Figure 3 Three nano droplet sizes (1500, 3000, and 6000 molecules) of water on the three-layer MoS_2 surface together with their representative top and side views.

Table 2 Non-bonded FF parameters describing interaction between water and the basal surface of three MoS_2 layers. Atomic charges of Mo and S are +0.50 and -0.25 e, respectively, taken from quantum chemical calculations.[28,44]

Interaction	Parameter	
	σ (nm)	ε (kJ/mol)
Mo-O	0.3000	0.0479
Mo-H	0.1500	0.0357
S-O	0.3020	1.4958
S-H	0.1870	0.0867

The predicted adsorption energy of water on MoS_2 using the new FF lies in the same range with the other two quantum-consistent FFs S3 and S4 (Table 1). Specifically, the S3 and S4 sets predicted adsorption energies of ~8.9 and 6.5 kJ/mol, respectively, and the new parameters predicted 7.8 kJ/mol, mid-way between the two. Intriguingly, this value is in good agreement with an estimate of 8.2 kJ/mol reported elsewhere.[29]

In summary, although all the FFs considered here could recover the experimental contact angle, not all FFs demonstrated consistent performance regarding the *ensemble* of microscopic configurations that ultimately underpins and confers this macroscopic property. In the case where the interfacial solvent structure matters, as for biomolecule adsorption, it is recommended to adopt the additional

evaluation criterion based on energetic ordering, provided this ordering can be benchmarked against robust approaches such as RPA. As proposed and tested here, application of this approach has yielded a new FF for molecular dynamics-based simulations of interfacial interaction between water and the MoS_2 basal plane which can fully meet these two criteria.

This work was supported by the Air Force Office of Scientific Research Grant FA9550-18-1-0329. Computational resources were provided by the National Computational Infrastructure (NCI), Canberra, and the Pawsey Supercomputing Centre, Perth, under the NCMAS scheme.

Conflicts of interest

There are no conflicts to declare.

References

1 T. T. Chau, W. J. Bruckard, P. T. L. Koh and A. V. Nguyen, *Adv. Colloid Interface Sci.*, 2009, **150**, 106–115.
2 W. A. Zisman, in *Contact Angle, Wettability, and Adhesion*, American Chemical Society, 1964, vol. 43, pp. 1–51.
3 N. Giovambattista, P. G. Debenedetti and P. J. Rossky, *J. Phys. Chem. B*, 2007, **111**, 9581–9587.
4 H. Li, T. Yan, K. A. Fichthorn and S. Yu, *Langmuir*, 2018, **34**, 9917–9926.
5 T. Koishi, K. Yasuoka, S. Fujikawa and X. C. Zeng, *ACS Nano*, 2011, **5**, 6834–6842.
6 J. E. Andrews, S. Sinha, P. W. Chung and S. Das, *Phys. Chem. Chem. Phys.*, 2016, **18**, 23482–23493.
7 J. Li and F. Wang, *J. Chem. Phys.*, 2017, **146**, 054702.
8 Y. Wu, L. K. Wagner and N. R. Aluru, *J. Chem. Phys.*, 2016, **144**, 164118.
9 A. Budi and T. R. Walsh, *Langmuir*, 2019, **35**, 16234–16243.
10 B. Luan and R. Zhou, *Appl. Phys. Lett.*, 2016, **108**, 131601.
11 V. Sresht, A. Govind Rajan, E. Bordes, M. S. Strano, A. A. H. Pádua and D. Blankschtein, *J. Phys. Chem. C*, 2017, **121**, 9022–9031.
12 J. Liu, J. Zeng, C. Zhu, J. Miao, Y. Huang and H. Heinz, *Chem. Sci.*, 2020, **11**, 8708–8722.
13 E. R. Cruz-Chu, A. Aksimentiev and K. Schulten, *J. Phys. Chem. B*, 2006, **110**, 21497–21508.
14 K. Liu, J. Feng, A. Kis and A. Radenovic, *ACS Nano*, 2014, **8**, 2504–2511.
15 A. B. Farimani, K. Min and N. R. Aluru, *ACS Nano*, 2014, **8**, 7914–7922.
16 M. Heiranian, A. B. Farimani and N. R. Aluru, *Nat. Commun.*, 2015, **6**, 8616.
17 S. Roobakhsh, Z. Rostami and S. Azizian, *Sep. Purif. Technol.*, 2018, **200**, 23–28.
18 Y. Zhou, X. Fan, G. Zhang and W. Dong, *Chem. Eng. J.*, 2019, **356**, 1003–1013.
19 K. Ai, C. Ruan, M. Shen and L. Lu, *Adv. Funct. Mater.*, 2016, **26**, 5542–5549.
20 Z. Wang and B. Mi, *Environ. Sci. Technol.*, 2017, **51**, 8229–8244.
21 D. J. Late, Y.-K. Huang, B. Liu, J. Acharya, S. N. Shirodkar, J. Luo, A. Yan, D. Charles, U. V. Waghmare, V. P. Dravid and C. N. R. Rao, *ACS Nano*, 2013, **7**, 4879–4891.
22 M. A. Islam, H. Li, S. Moon, S. S. Han, H.-S. Chung, J. Ma, C. Yoo, T.-J. Ko, K. H. Oh, Y. Jung and Y. Jung, *ACS Appl. Mater. Interfaces*, 2020, **12**, 53174–53183.
23 B. Radisavljevic, A. Radenovic, J. Brivio, V. Giacometti and A. Kis, *Nat. Nanotechnol.*, 2011, **6**, 147–150.
24 D. Lembke, S. Bertolazzi and A. Kis, *Acc. Chem. Res.*, 2015, **48**, 100–110.
25 V. Varshney, S. S. Patnaik, C. Muratore, A. K. Roy, A. A. Voevodin and B. L. Farmer, *Comput. Mater. Sci.*, 2010, **48**, 101–108.
26 J.-W. Jiang, H. S. Park and T. Rabczuk, *J. Appl. Phys.*, 2013, **114**, 064307.
27 T. Liang, S. R. Phillpot and S. B. Sinnott, *Phys. Rev. B*, 2009, **79**, 245110.
28 M. Heiranian, Y. Wu and N. R. Aluru, *J. Chem. Phys.*, 2017, **147**, 104706.
29 F. Leroy, *J. Chem. Phys.*, 2016, **145**, 164705.
30 Z. Gu, P. De Luna, Z. Yang and R. Zhou, *Phys. Chem. Chem. Phys.*, 2017, **19**, 3039–3045.
31 A. A. Skelton, T. Liang and T. R. Walsh, *ACS Appl. Mater. Interfaces*, 2009, **1**, 1482–1491.
32 K. Lee, É. D. Murray, L. Kong, B. I. Lundqvist and D. C. Langreth, *Phys. Rev. B*, 2010, **82**, 081101.
33 P. Giannozzi, O. Andreussi, T. Brumme, O. Bunau, M. Buongiorno Nardelli, M. Calandra, R. Car, C. Cavazzoni, D. Ceresoli, M. Cococcioni, N. Colonna, I. Carnimeo, A. Dal Corso, S. de Gironcoli, P. Delugas, R. A. DiStasio, A. Ferretti, A. Floris, G. Fratesi, G. Fugallo, R. Gebauer, U. Gerstmann, F. Giustino, T. Gorni, J. Jia, M. Kawamura, H.-Y. Ko, A. Kokalj, E. Küçükbenli, M. Lazzeri, M. Marsili, N. Marzari, F. Mauri, N. L. Nguyen, H.-V. Nguyen, A. Otero-de-la-Roza, L. Paulatto, S. Poncé, D. Rocca, R. Sabatini, B. Santra, M. Schlipf, A. P. Seitsonen, A. Smogunov, I. Timrov, T. Thonhauser, P. Umari, N. Vast, X. Wu and S. Baroni, *J. Phys.: Condens. Matter*, 2017, **29**, 465901.
34 M. J. Abraham, T. Murtola, R. Schulz, S. Páll, J. C. Smith, B. Hess and E. Lindahl, *SoftwareX*, 2015, **1–2**, 19–25.
35 C. González, B. Biel and Y. J. Dappe, *Phys. Chem. Chem. Phys.*, 2017, **19**, 9485–9499.
36 S. Zhao, J. Xue and W. Kang, *Chem. Phys. Lett.*, 2014, **595–596**, 35–42.
37 W. L. Jorgensen, J. Chandrasekhar, J. D. Madura, R. W. Impey and M. L. Klein, *J. Chem. Phys.*, 1983, **79**, 926–935.
38 H. J. C. Berendsen, J. R. Grigera and T. P. Straatsma, *J. Phys. Chem.*, 1987, **91**, 6269–6271.
39 A. D. MacKerell, D. Bashford, M. Bellott, R. L. Dunbrack, J. D. Evanseck, M. J. Field, S. Fischer, J. Gao, H. Guo, S. Ha, D. Joseph-McCarthy, L. Kuchnir, K. Kuczera, F. T. K. Lau, C. Mattos, S. Michnick, T. Ngo, D. T. Nguyen, B. Prodhom, W. E. Reiher, B. Roux, M. Schlenkrich, J. C. Smith, R. Stote, J. Straub, M. Watanabe, J. Wiórkiewicz-Kuczera, D. Yin and M. Karplus, *J. Phys. Chem. B*, 1998, **102**, 3586–3616.
40 S. Piana, K. Lindorff-Larsen and D. E. Shaw, *Biophys. J.*, 2011, **100**, L47–L49.
41 E. Neria, S. Fischer and M. Karplus, *J. Chem. Phys.*, 1996, **105**, 1902–1921.
42 T. Werder, J. H. Walther, R. L. Jaffe, T. Halicioglu and P. Koumoutsakos, *J. Phys. Chem. B*, 2003, **107**, 1345–1352.
43 A. Kozbial, X. Gong, H. Liu and L. Li, *Langmuir*, 2015, **31**, 8429–8435.
44 V. Sresht, A. Govind Rajan, E. Bordes, M. S. Strano, A. A. H. Pádua and D. Blankschtein, *J. Phys. Chem. C*, 2017, **121**, 9022–9031.

